American Journal of Optics and Photonics
2019; 7(1): 10-17
http://www.sciencepublishinggroup.com/j/ajop
doi: 10.11648/j.ajop.20190701.12
ISSN: 2330-8486 (Print); ISSN: 2330-8494 (Online)

Germanium Based Two-Dimensional Photonic Crystals with Square Lattice

Fairuz Aniqa Salwa, Muhammad Mominur Rahman, Muhammad Obaidur Rahman, Muhammad Abdul Mannan Chowdhury

Department of Physics, Jahangirnagar University, Savar, Dhaka, Bangladesh

Email address:
mmrahman.phy@gmail.com (M. M. Rahman)

To cite this article:
Fairuz Aniqa Salwa, Muhammad Mominur Rahman, Muhammad Obaidur Rahman, Muhammad Abdul Mannan Chowdhury. Germanium Based Two-Dimensional Photonic Crystals with Square Lattice. *American Journal of Optics and Photonics.* Vol. 7, No. 1, 2019, pp. 10-17. doi: 10.11648/j.ajop.20190701.12

Received: March 11, 2019; **Accepted**: April 26, 2019; **Published**: May 15, 2019

Abstract: Using the plane-wave expansion method, we study the polarization-dependent photonic band diagrams (transverse electric and transverse magnetic polarizations), surface plots, gap maps etc. of the two-dimensional photonic crystals with square lattice of germanium rods in air and vice versa. The obtained graphs for the two possible combinations are presented in this paper. All the results depict clear photonic band gaps. We describe the conditions for the largest TE and TM band gaps too. The square lattice of Ge rods in air offers a large TE photonic band gap of 48.02% (for rod radius of r = 0.2μm). Then we localize the TE mode by introducing a point defect and a line defect in the crystal. The point defect act as a resonator and the line defect act as a waveguide. The finite-difference time-domain analysis of the localized defect modes is presented also.

Keywords: Photonic Crystals, Transverse Electric Modes, Transverse Magnetic Modes, Plane Wave Expansion Method, Finite Difference Time Domain Method, Photonic Band Diagram, Gap Map, Square Lattice

1. Introduction

Recently intensive researches have been carried out on photonic crystals (PCs) [1–5] as they hold great promise for optoelectronic devices owing the ability to control electromagnetic wave propagation within a fairly large frequency range. They are novel class of optical media with periodic variation of the refractive index in one, two or three dimensions. Yablonovitch gave the concept of PC first [4] as a medium that inhibit spontaneous emission of electromagnetic radiation. Analogous to the solid crystal's electronic band gap, PC prohibits the propagation of electromagnetic radiation of certain frequency range through it [3, 6, 7]. The crystal is said to have a photonic band gap (PBG). In such a photonic crystal, no light modes can propagate if the frequency of light is within that PBG range.

However, if a defect is introduced into this crystal, new eigen-state with energy corresponding to the eigen-frequency of the defect appears inside the PBG. Thus, light having the defect frequency will propagate along the defect through the crystal. In this way, we may create a waveguide that guides light from one location to another. Once light is induced to travel along this waveguide carved in photonic crystal, it has nowhere else to go as the mode is forbidden to escape into the crystal.

In this paper, a two-dimensional (2D) photonic crystal with square lattice of Ge rods in air as well as air holes in Ge has been considered. The shape and size of the PBG are shown and the effects of different parameters on the PBG like rod radius or hole radius, filling fraction etc. have been investigated. The photonic band structure calculation was performed using the RSoft software package "BandSOLVE", which is based on the plane wave expansion (PWE) method.

Finally, we introduce a point defect and a line defect in the 2D PC with square lattice of Ge rods in air by removing the central rod and a line of rods from the crystal respectively. Subsequently, the effects of these defects on the crystal have been discussed. The defect modes are calculated using the RSoft software package "FullWAVE", which is based on the finite-difference time-domain (FDTD) method.

2. Theoretical Background

2.1. The Plane-Wave Expansion Method

The electromagnetic modes are governed by the master equations for the electric field and that for the magnetic field. They are given by:

$$\widehat{\mathbb{C}}_E E(r) \equiv \frac{1}{\varepsilon(r)} \nabla \times \{\nabla \times E(r)\} = \frac{\omega^2}{c^2} E(r), \quad (1)$$

$$\widehat{\mathbb{C}}_H H(r) \equiv \nabla \times \left\{\frac{1}{\varepsilon(r)} \nabla \times H(r)\right\} = \frac{\omega^2}{c^2} H(r). \quad (2)$$

Where, $\varepsilon(r)$ is a periodic dielectric function, c is the speed of light, $E(r)$ and $H(r)$ are the electric and magnetic field of an electromagnetic mode of frequency ω, c is the speed of light and the two differential operators $\widehat{\mathcal{L}}_E$ and $\widehat{\mathcal{L}}_H$ are defined by the first equality in each of the above equations.

Because of the periodicity of the dielectric function $\varepsilon(r)$, we can expand the inverse of the dielectric function ε^{-1}(r) in a Fourier series of plane waves [8] of the form:

$$\xi(r) = \frac{1}{\varepsilon(r)} = \sum_G \kappa(G)\, e^{iG.r} \quad (3)$$

Where, G is the reciprocal lattice vector.

Now using the Bloch's theorem and expanding the eigenfunctions in Fourier series, we finally obtain the following equations:

$$-\sum_{G'} \kappa(G - G')\,(k + G') \times \left\{(k + G') \times E_{kn}(G')\right\} = \frac{\omega_{kn}^2}{c^2} E_{kn}(G), \quad (4)$$

$$-\sum_{G'} \kappa(G - G')\,(k + G) \times \left\{(k + G') \times H_{kn}(G')\right\} = \frac{\omega_{kn}^2}{c^2} H_{kn}(G). \quad (5)$$

This numerical method is called the plane-wave expansion method. By solving one of these two sets of equations (4) and (5) numerically, we can obtain the dispersion relation of the eigenmodes, or the photonic band structure [9, 10].

2.2. The Finite-Difference Time-Domain (FDTD) Method

The FDTD method or Yee's method is one of the most advanced numerical analysis techniques today for computation of the field distribution inside the PC-based devices. Briefly, it divides the three-dimensional problem geometry into Yee cells to form a grid [11]. The Yee algorithm solves for both electric and magnetic fields in time and space using the coupled Maxwell's curl equations. It centers its E and H components in three-dimensional space so that every E component is surrounded by four circulating H components, and every H component is surrounded by four circulating E components. This provides a beautifully simple picture of three-dimensional space being filled by an interlinked array of Faraday's law and Ampere's law contours. The Yee algorithm also centers its E and H components in time in a leapfrog arrangement [11]. After that, derivatives in Maxwell's equations are replaced by finite differences that results in a system of algebraic equations which are linear on coordinates.

We consider that our modelled 2D structure is periodic along xz-plane and extends to infinity in the y-direction with no change in the shape or position of its transverse cross section. The incident wave is also uniform in the y-direction. Under these conditions, the full set of Maxwell's curl equations are given by:

$$\frac{\partial H_x}{\partial t} = \frac{1}{\mu}\left[\frac{\partial E_y}{\partial z} - (M_x + \sigma^* H_x)\right], \quad (6)$$

$$\frac{\partial H_y}{\partial t} = \frac{1}{\mu}\left[\frac{\partial E_z}{\partial x} - \frac{\partial E_x}{\partial z} - (M_y + \sigma^* H_y)\right], \quad (7)$$

$$\frac{\partial H_z}{\partial t} = \frac{1}{\mu}\left[-\frac{\partial E_y}{\partial x} - (M_z + \sigma^* H_z)\right], \quad (8)$$

$$\frac{\partial E_x}{\partial t} = \frac{1}{\varepsilon}\left[-\frac{\partial H_y}{\partial z} - (J_x + \sigma E_x)\right], \quad (9)$$

$$\frac{\partial E_y}{\partial t} = \frac{1}{\varepsilon}\left[\frac{\partial H_x}{\partial z} - \frac{\partial H_z}{\partial x} - (J_y + \sigma E_y)\right], \quad (10)$$

$$\frac{\partial E_z}{\partial t} = \frac{1}{\varepsilon}\left[\frac{\partial H_y}{\partial x} - (J_z + \sigma E_z)\right] \quad (11)$$

Where, J is the electric current density (amperes / meter^2), M is the equivalent magnetic current density (volts / meter^2), ε is the electric permittivity (farads / meter), μ is the magnetic permeability (henrys / meter), σ is the electric conductivity (siemens / meter) and σ^* is the equivalent magnetic loss (ohms / meter).

There are two types of modes in case of 2D electromagnetic wave interaction problems:

1. Transverse-Magnetic (TM) Mode

At first, let us group equations (7), (9), and (11), which involve only H_y, E_x and E_z. We will denote this set of field components the transverse-magnetic (TM) mode in two dimensions.

2. Transverse-Electric (TE) Mode

Secondly, let us group equations (6), (8) and (10), which involve only H_x, H_z and E_y. We will designate this set of field components the transverse-electric (TE) mode in two dimensions.

There are no common field vector components in between the TM and TE modes. Thus, these modes can exist simultaneously with no mutual interactions for structures composed of isotropic materials or anisotropic materials having no off-diagonal components in the constitutive tensors. These two modes may have very different physical phenomena associated with them.

3. Results and Discussions

3.1. Square Lattice of Germanium Rods in Air

We consider a two-dimensional square array of germanium rods (refractive index, n_1 = 4.45) having circular cross-

section embedded in an air background (refractive index, $n_2 = 1$) as shown in figure 1(a). The crystal is periodic along the xz-plane and homogeneous along the y-direction. The radius of the Ge cylinders is, r = 0.2 μm and the lattice constant is, a = 1 μm. So, the relative radius [12] is, $\frac{r}{a} = 0.2$ and the filling factor is, $f = 0.126$.

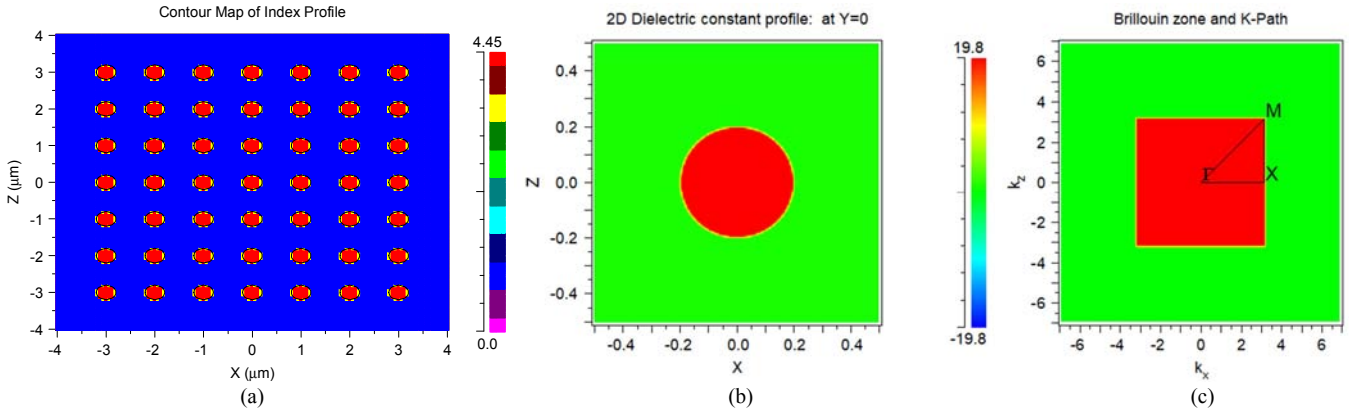

(a) (b) (c)

Figure 1. *(a) A two-dimensional (2D) photonic crystal with square lattice consisting of germanium rods in air that was designed in the Rsoft CAD layout, (a) a single unit cell for this lattice and (b) the Brillouin zone for this lattice. Γ, X and M are the high symmetry points in the triangular irreducible Brillouin zone.*

This 2D square lattice array has a square Brillouin zone with an irreducible Brillouin zone as shown in figure 1(c). The irreducible Brillouin zone is the triangular wedge in the upper-right corner; the rest of the Brillouin zone can be related to this wedge by rotational symmetry. This irreducible Brillouin zone is used to explain light propagation in the photonic crystal. In figure 1(c), k_x and k_z represent the wave vectors along x and z-directions. The high symmetry points in the triangular irreducible Brillouin zone are defined as Γ, X and M with coordinate axis Γ(0, 0), X(π/a, 0) and M(π/a, π/a).

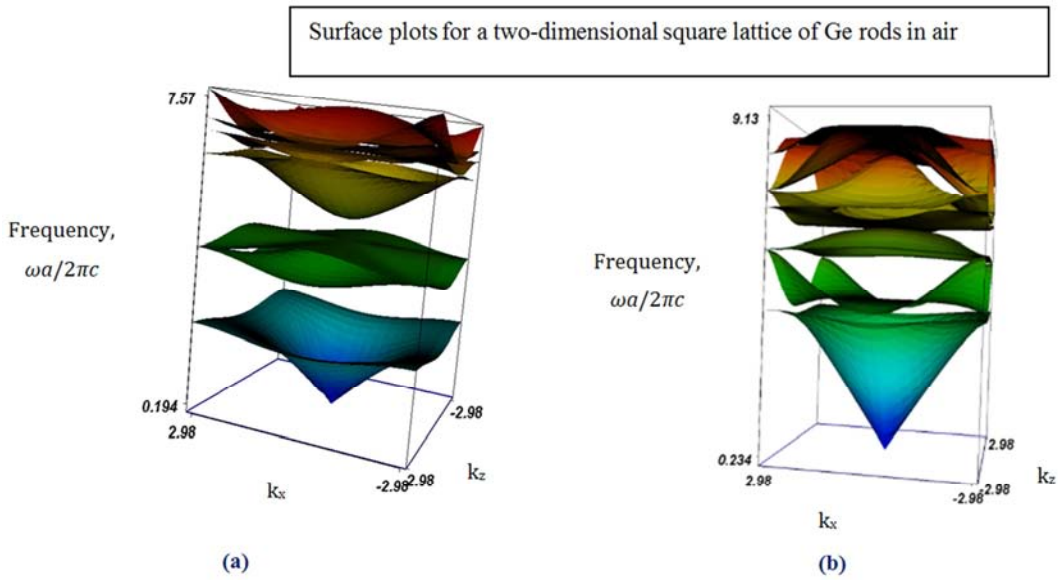

Figure 2. *Surface plots for the two-dimensional square lattice of Ge rods in air for (a) TE polarization and (b) TM polarization.*

Figure 2 shows the dispersion relation of this periodic structure as the surface plots for all in plane wave vectors $k_{||}$ in the irreducible Brillouin zone. We use plane wave expansion method [10, 13–16] for this calculation. The surface plots are classified into the TE and the TM polarizations. As can be seen from figure 2, there are two clear TE band gaps, but no band gap for TM polarization. We have the real view of the photonic band gaps from these plots. The definitions of TE and TM are given in [17].

Studying surface plots is hard quantitatively. Therefore, instead of studying the dispersion relation in the whole irreducible Brillouin zone, we will only look at it along the edges at Γ, X and M points. In this way, we can get clear photonic band diagrams for both TE and TM polarizations. They are plotted in figure 3(a). Along the vertical axis of the band diagram, the frequency is shown as a dimensionless ratio $\omega a/2\pi c$. The horizontal axis shows the value of the in plane wave vector $k_{||}$. As we move from left to right, $k_{||}$ moves along the triangular edge of the irreducible Brillouin zone, from Γ to X to M, as shown in figure 3(a).

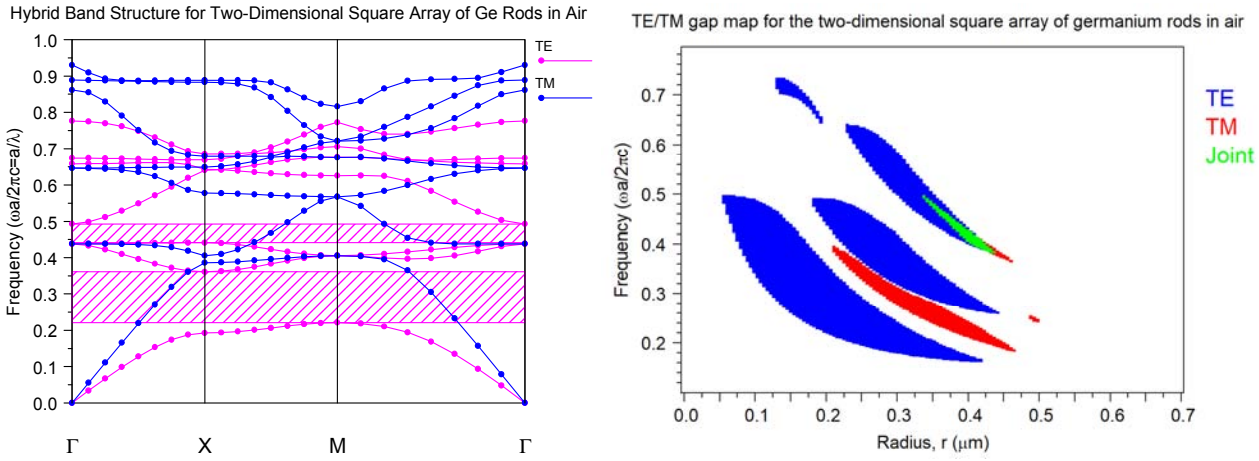

(a) (b)

Figure 3. *The TE and TM both or hybrid band structure for the two-dimensional square lattice of germanium cylinders in air. Due to the high index contrast, a wide gap opens between the first and second band for TE polarization. For TM polarization, no band gap is observed. (b) The gap map for this structure.*

The most striking aspect of figure 3(a) is the large TE gap between the first and second bands, with a gap/midgap ratio of about 48.02%. We denote this first TE band-gap as TE-1 band-gap. The TE-1 band-gap extends from $\omega = 0.22157(2\pi c/a)$ to $\omega = 0.35918(2\pi c/a)$. There is also a small band-gap between the third and fourth TE bands. We denote this second band-gap as TE-2 band-gap. The TE-2 band-gap extends from $\omega = 0.44106(2\pi c/a)$ to $\omega = 0.49293(2\pi c/a)$. No propagating TE waves are allowed in this frequency range, regardless of the wave-vector. However, there is no TM bandgap for this type of lattice. This can be explained by considering the polarization convention. For TE polarization, the external electric field is directed along the y-axis along which the Ge cylinder is considered to be infinitely long. That is why, the cylinder is easily polarized resulting in a strong interaction of the cylinder with TE polarized waves, whereas for TM polarization the polarizability of the cylinder is small. The band-gap width, mid-gap frequency, gap-midgap ratio and gap percentage for this structure are given in table 1.

Table 1. *TE Band Gap Data for The Two-Dimensional Photonic Crystal with Square Lattice of Ge rods in Air.*

Crystal structure	Band	$\frac{\omega a}{2\pi c}$	The mid-gap frequency of the gap (ω_m)	Band-gap width ($\Delta\omega$)	Gap-midgap ratio ($\Delta\omega/\omega_m$)	Gap-percentage (%)
Square lattice of Ge rods in air	1st	0.22157-0.35918	0.2910664648188	0.1397780188967	0.4802271501243	48.02
	2nd	0.44106-0.49293	0.4669885025237	0.05174092701029	0.1107970040604	11.08

Atlas of the Band Gaps

The radius of the dielectric cylinders plays an important role in determining the exact location and width of the gap. That is why, we vary the radius of the Ge rods, r and plot the corresponding variation of the photonic band gap size - which is known as the gap map [6]. Figure 3(b) shows the gap map for this lattice. The locations of the band gaps are outlined for the TE and TM polarizations using blue and red colours respectively. The overlap of TE and TM mode is shown using green colour.

From this gap map, we find many interesting properties of this photonic crystal. With the increase of the radius r, the gaps are decreased in frequency. TE band gap opens up at a radius of r = 0.056915 μm. As the radius of the rods is increased, a TM band-gap appears first at r = 0.2087 μm. Further increasing the radius causes the TE and TM band-gaps to overlap, resulting in a complete band-gap [6] i.e. a set of frequencies in which light of any polarization cannot propagate in any in-plane direction. The complete band-gap appears at r = 0.3349 μm. Although the plot extends from r = 0 to r = 0.7 μm, all of the gaps seal up by the time r = 0.50 μm. At that value, the Ge rods touch one another. The gap width decreases with the increase of the radius. The largest TE band-gap occurs at r = 0.15954 μm. The largest TM band-gap occurs at r = 0.35464 μm. The largest complete band-gap occurs at r = 0.40191 μm. Its width is only $\Delta\omega = 0.025561(2\pi c/a)$.

3.2. Square Lattice of Air Holes in Germanium

A two-dimensional square photonic crystal lattice composed of circular air holes in germanium with r/a = 0.2 is considered as shown in figure 4(a).

The resulting band diagrams for TE and TM polarizations for this structure are plotted in figure 4(b). There is no band gap for any polarization for this value of the radius and refractive index contrast. This lattice can not prohibit EM wave propagation through it and is therefore transparent.

But as we varied the radius of the air holes, r from 0 μm to 0.7 μm, we found that band gap appears for both polarizations as shown in the gap map of figure 4(c). The gap map shows several important properties. At first, a TM band gap seems to open up around the radius of r = 0.31406 μm. Then a TE band gap appears for r = 0.39748 μm. Also a thin complete photonic band gap appears for r = 0.46912 μm. With the increase of the radius r, the gap frequency is

increased. The gap width also increases with the increase of radius r. The widest TE band gap occurs at r = 0.59027 μm. The widest TM band gap occurs at r = 0.49196 μm. The widest complete band gap occurs at r = 0.492 μm. Its width is only $\Delta\omega = 0.028702(2\pi c/a)$. At the radius of about 0.4 μm, there are four TM band gap and one TE band gap. This is just opposite to the case of germanium rods in air. As we reverse the crystal structure of square lattice of germanium rods in air by inserting air pores into germanium, we get the opposite result.

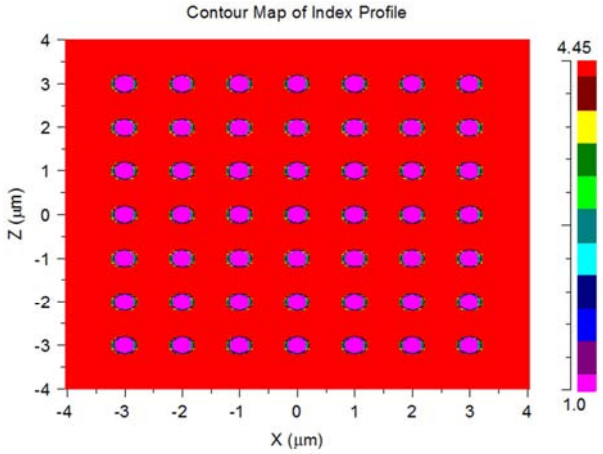

(a)

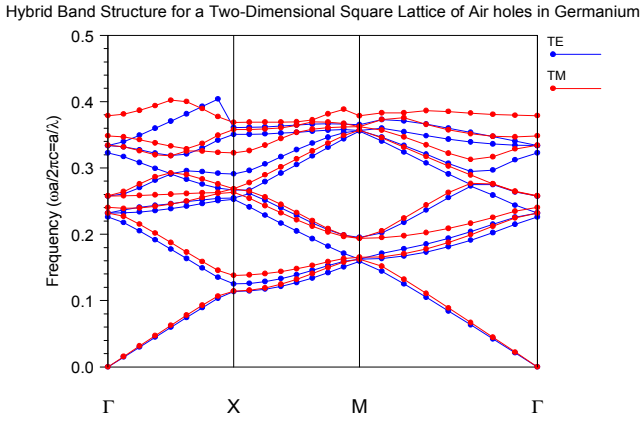

(b)

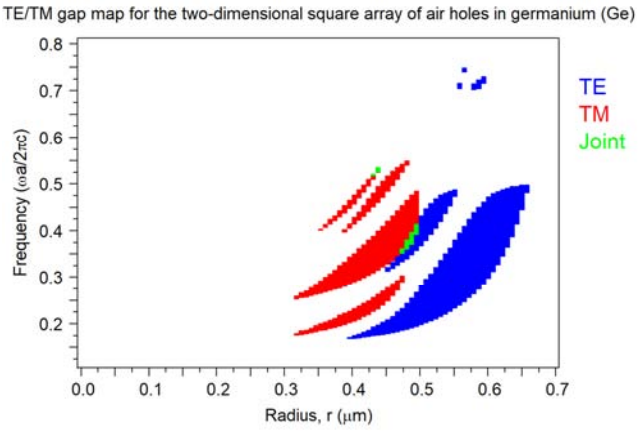

(c)

Figure 4. *(a) The refractive index profile for the two-dimensional (2D) square lattice consisting of air holes in germanium that was designed in the Rsoft CAD layout, (b) the TE and TM both or hybrid band structure for this structure and (c) the gap map for this structure.*

3.3. Point Defects in Two-Dimensional Photonic Crystals

A point defect is introduced in the 2D square lattice composed of germanium rods in air by removing one germanium rod from the center of the crystal as shown in figure 5.

The numerical simulation of the defect cavity is performed using the plane-wave expansion method (PWE). We use a 7 × 7 square supercell to find the defect mode as shown in figure 5(a). The defect state is found to exist at the 48th band as shown in figure 5(b). The straight band inside the photonic band gap represents the defect state [18]. This defect has the symmetry of the C_{4v} point group [8]. Here, we simulated the TE mode. Because we found two TE band gaps and no TM band gap for the square lattice of germanium rods in air.

The results of the mode computation are shown in figure 6. The defect in this square array introduces a localized mode at the defect site, as shown in these figures. The defect mode cannot penetrate into the rest of the crystal, since it has a frequency in the band gap. So, defect modes decay exponentially in the crystal. They are localized in the xz plane, but extend in the y direction.

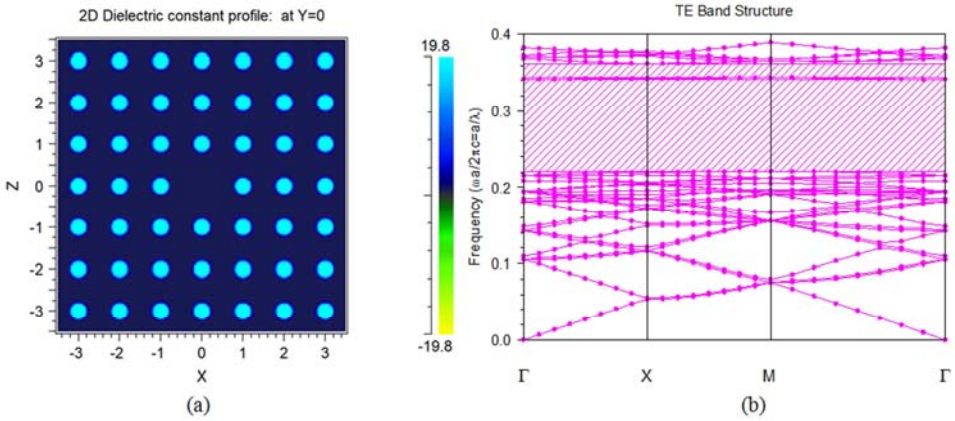

(a) (b)

Figure 5. *(a) A supercell containing a point defect in the 2D square lattice of germanium (Ge) rods in air. The point defect was introduced in the crystal lattice by removing one germanium rod from the center. (b) TE band diagram for this defective crystal lattice. The straight band inside the photonic band gap represents the defect state.*

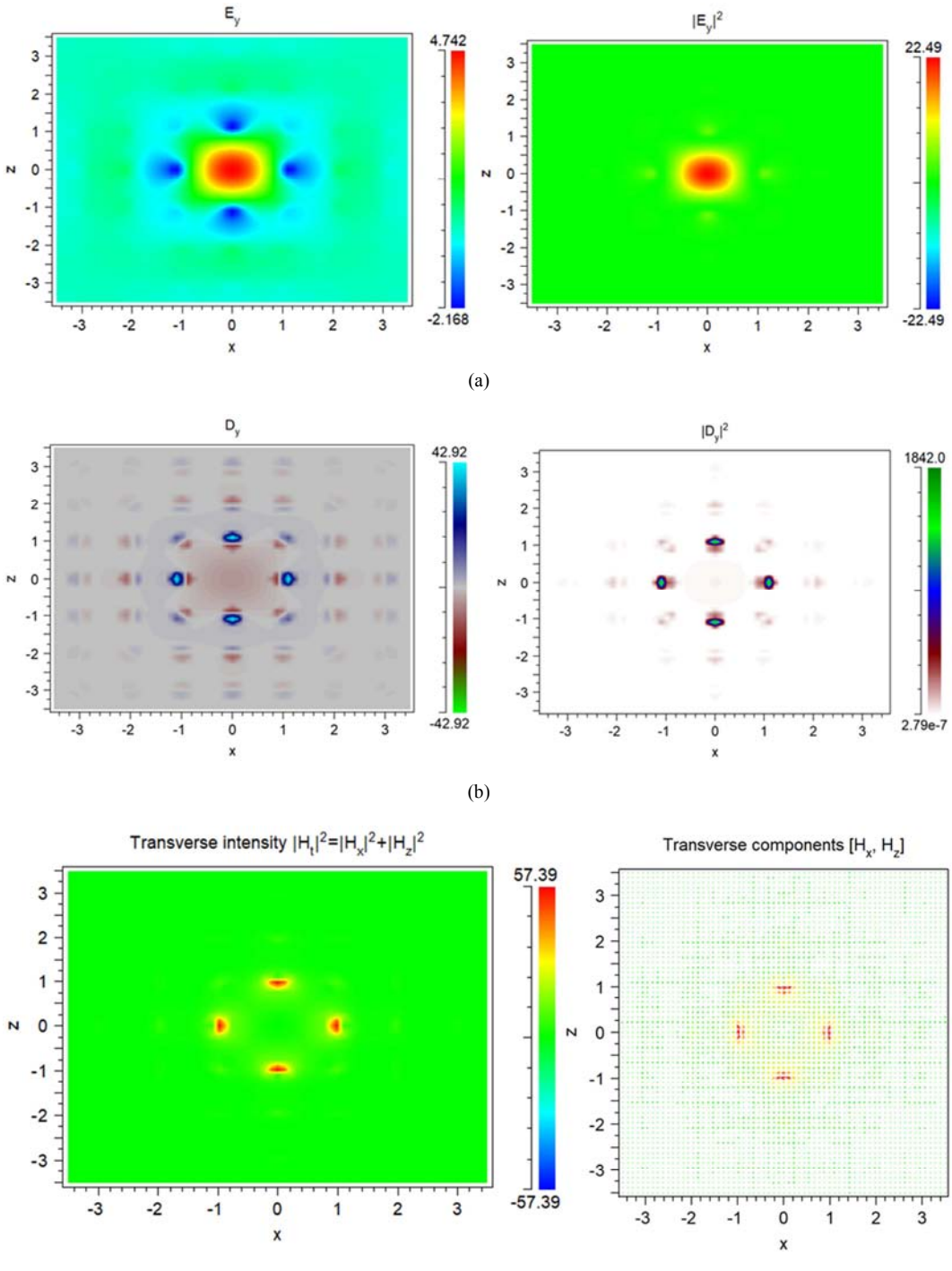

Figure 6. *Localization of the (a) electric field (E_y), (b) displacement field (D_y) and (c) transverse component of the magnetic field (H_x and H_z) in the point defect in the two-dimensional (2D) square lattice of germanium rods in air.*

Therefore, this PC may be used as a resonator in different optical devices.

3.4. Line Defects in Two-Dimensional Photonic Crystals and Waveguides

Next, we introduce a line defect in the two-dimensional (2D) square lattice of germanium rods in air by removing a column of germanium rods from the crystal. We simulate the propagation of electromagnetic waves having wavelength λ = 1.5 μm using the finite-difference time-domain method (FDTD) with perfectly-matched-layer (PML) boundary conditions. Ten grid points per wavelength are used. A light source located at the entrance of the input waveguide create a pulse with a Gaussian envelope in time. The field amplitude is monitored by inserting a time monitor at the end of the waveguide, as indicated by the black rectangle at the top of figure 8. We used the 'FullWAVE' software to do this simulation. The simulation results are shown in figure 8.

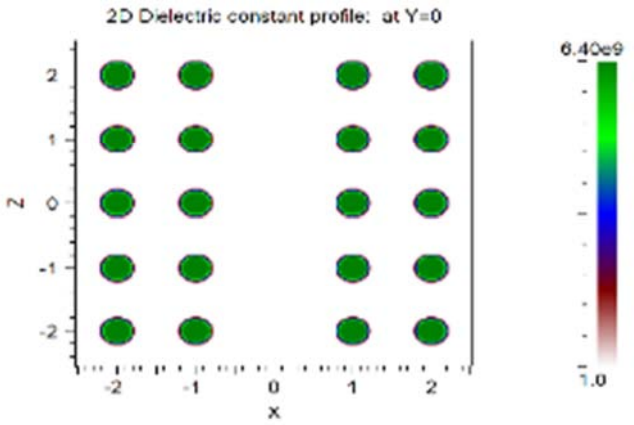

Figure 7. *A line defect in the two-dimensional (2D) square lattice of germanium rods in air.*

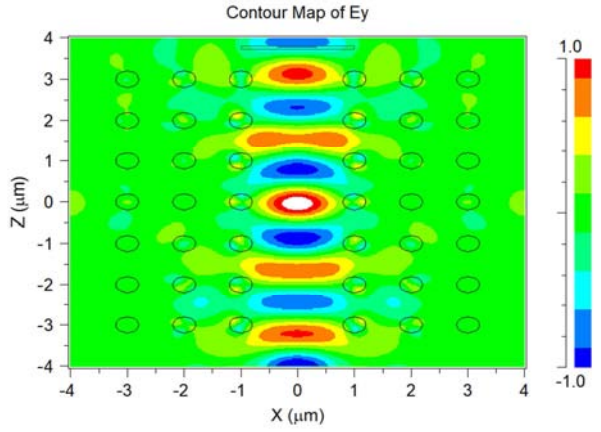

(a)

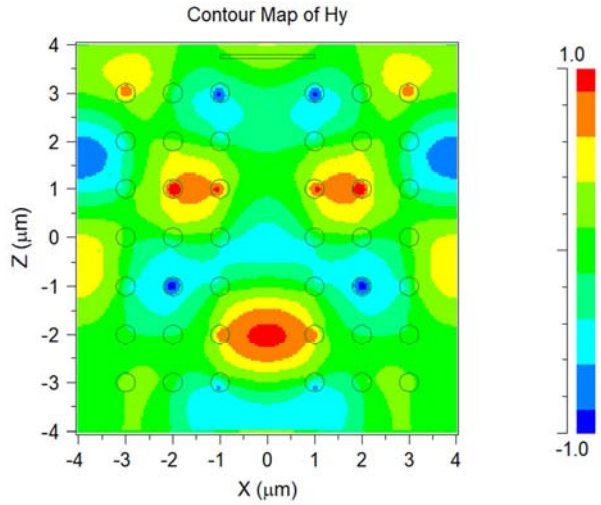

(b)

Figure 8. *(a) Electric field component E_y of the localized TE mode and (b) magnetic field component H_y of the unlocalized TM mode. Red and blue represent positive and negative fields, while green represents zero field. The Ge rods are shown as black outlines.*

We consider both the TE and TM polarizations. In the case of TE light, the incoming light's frequency lies within a photonic bandgap of the crystal. Since light cannot propagate in the crystal if its wavelength falls inside a bandgap, the only possibility for the TE light is to follow the waveguides created by the missing rods. Thus, we have the localized TE mode within the defect, as shown in figure 8(a). For the case of TM polarization, it happens that the structure does not support a bandgap at all, so there is no chance of photonic bandgap guidance. Thus, the TM mode is not localized within the crystal, as shown in figure 8(b).

4. Conclusion

We considered 2D PC with square lattice of Ge rods in air as well as air holes in Ge and showed the corresponding photonic band diagrams. The actual view of the photonic band gaps are presented. We obtained a large TE band gap with a gap-percentage of 48.02% for the square lattice of Ge rods in air. Finally, we applied this data successfully to design a waveguide.

We analyzed the defect modes of a 2D photonic crystal having a point defect and a line defect, using the finite-difference time domain (FDTD) method. We observed that, introducing defects in two-dimensional photonic crystals permits us to localize and guide light having frequencies in the photonic band gap. It is impossible for that light to propagate in the crystal. The only way for the light is to propagate through the defect. Therefore, this 2D photonic crystal is very convenient for use as a cladding of photonic crystal fiber and promising candidates for various photonic device designs such as resonators, laser cavities, filters, waveguides, sensors and other novel integrated optics applications.

Acknowledgements

The authors thank the Information and Communication Technology Division (ICT- Division), Department of the Ministry of Posts, Telecommunications and Information Technology of the Government of Bangladesh, for providing the prestigious ICT fellowship 2017-18 (2nd round) and supporting this research work.

References

[1] F. Wen, S. David, X. Checoury, M. El Kurdi, and P. Boucaud, "Two-dimensional photonic crystals with large complete photonic band gaps in both TE and TM polarizations," *Opt. Express*, 16, 12278 (2008).

[2] E. Yablonovitch, "Photonic crystals: What's in a Name?," Opt. Photonics News, 18, 12–13 (2007).

[3] E. Yablonovitch, "Photonic Band-Gap Crystals," J. Physics-Condensed Matter, 5, 2443–2460 (1993).

[4] E. Yablonovitch, "Inhibited spontaneous emission in solid-state physics and electronics," Phys. Rev. Lett., 58, 2059–2062 (1987).

[5] K. Arunachalam and S. C. Xavier, "Optical Logic Devices Based on Photonic Crystal," *Intech* (2010).

[6] J. D. Joannopoulos, S. G. Johnson, J. N. Winn, and R. D. Meade, *Photonic crystals: molding the flow of light*, 2nd ed. (Princeton University Press, 2008).

[7] I. A. Sukhoivanov and I. V. Guryev, *Photonic Crystals Physics and Practical Modeling* (Springer, 2005).

[8] M. Skorobogatiy and J. Yang, *Fundamentals of Photonic Crystal Guiding* (Cambridge, 2008).

[9] J. D. Joannopoulos, J. N. Winn, and R. D. Meade, *Photonic crystals: molding the flow of light*, 1st ed. (Princeton University Press, 1995).

[10] S. McCall, P. Platzman, R. Dalichaouch, D. Smith, and S. Schultz, "Microwave propagation in two-dimensional dielectric lattices," *Phys. Rev. Lett.*, vol. 67, no. 15, pp. 2017–2020, Oct. 1991.

[11] A. Taflove, S. C. Hagness, and K. S. Yee, *Computationai Electrodynamics: The Finite-Difference Time-Domain Method*, vol. 14, no. 3. 1966.

[12] D. J. Griffiths, *Introduction to Electrodynamics*, Third edit. Prentice-Hall, 1999.

[13] S. Shi, C. Chen, and D. W. Prather, "Plane-wave expansion method for calculating band structure of photonic crystal slabs with perfectly matched layers," *J. Opt. Soc. Am. A*, vol. 21, no. 9, p. 1769, 2004.

[14] R. Antos and M. Veis, "Fourier Factorization in the Plane Wave Expansion Method in Modeling Photonic Crystals," in *Photonic Crystals - Introduction, Applications and Theory*, no. 1, 2012, pp. 319–344.

[15] C. Jamois, R. B. Wehrspohn, L. C. Andreani, C. Hermann, O. Hess, and U. Gösele, "Silicon-based two-dimensional photonic crystal waveguides," *Photonics Nanostructures - Fundam. Appl.*, vol. 1, no. 1, pp. 1–13, 2003.

[16] Kazuaki Sakoda, "*Optical Properties of Photonic Crystals*", 2nd ed., (Springer 2005).

[17] Salwa, F. A., Rahman, M. M., Rahman, M. O. and Chowdhury, M. A. M. (2019) Germanium Based Two-Dimensional Photonic Crystals: The Hexagonal and Honeycomb Lattices. Optics and Photonics Journal, 9, 25-36. https://doi.org/10.4236/opj.2019.93004.

[18] K. M. Ho, C. T. Chan, and C. M. Soukoulis, "Existence of a photonic gap in periodic dielectric structures," *Phys. Rev. Lett.*, vol. 65, no. 25, 1990.